# Keystone bacterial functional module activates P-mineralizing genes to enhance enzymatic hydrolysis of organic P in a subtropical forest soil with 5-year N addition

Quanxin Zeng[1,2,3], Josep Peñuelas[4, 5], Jordi Sardans[4, 5], Qiufang Zhang[1,2], Jiacong Zhou[1,2], Kai Yue [1,2,3], Yuehmin Chen [1,2,3*], Yusheng Yang[1,2,3], Yuexin Fan[1,2,3*]

**Affiliations:**

[1] State Key Laboratory for Subtropical Mountain Ecology of the Ministry of Science and Technology and Fujian Province, Fujian Normal University, Fuzhou 350007, China

[2] School of Geographical Sciences, Fujian Normal University, Fuzhou 350007, China

[3] Institute of Geography, Fujian Normal University, Fuzhou 350007, China

[4] CREAF, E08193 Cerdanyola del Vallès, Catalonia, Spain

[5] CSIC, Global Ecology Unit, CREAF-CSIC-UAB, E08193 Cerdanyola del Vallès, Catalonia, Spain

[*]**Corresponding author:** Yuehmin Chen and Yuexin Fan

**Email:** ymchen@fjnu.edu.cn (Yuehmin Chen); yxfan@fjnu.edu.cn (Yuexin Fan)

**Post address:** Shangsan Road 8, Cangshan District, Fuzhou 350007, Fujian, China

## Abstract

Microorganisms play an integral role in driving P transformation in forest soils; however, studies on soil P cycling and the molecular mechanisms of microbes activated in response to elevated nitrogen (N) deposition are limited. In this study, we conducted a multilevel field N enrichment experiment in a subtropical P-deficient Moso bamboo (*Phyllostachys heterocycla*) system to evaluate the microbial ecological traits of P transformation (e.g., organic P mineralization and inorganic P solubilization) over three consecutive years. N addition significantly decreased available and organic P levels in the soil and increased the microbial biomass C:P and N:P ratios, indicative of severe microbial P limitation. Consequently, N addition increased the absolute abundance of P starvation response regulation genes (*phoU* and *phoR*), which further induced an increase in organic P mineralization (*phoN*, *phoD*, *appA*), but not that of inorganic P solubilization genes (*ppx* and *gcd*). This suggests that microbes enhance P availability by organic P mineralization rather than inorganic P solubilization to ameliorate reduced P availability. Furthermore, a bacterial functional module (B_Mod#0) consisting of *Proteobacteria*, *Actinobacteria*, and *Firmicutes* accounted for more than 60% of the changes in the abundance of genes responsible for organic P-mineralization in the soil, suggesting that B_Mod#0 acts as a keystone phylotype in enhancing functional P-cycling potential. This study provides novel insights into microorganism-driven P cycling in P-deficient forest soils with N addition.



**Keywords:** Nitrogen deposition, Phosphorus limitation, Microbial modules, Functional P-cycling potential, Phosphorus mineralization

## 1. Introduction

Over the past century, the increase in N deposition has resulted in a global N/P imbalance caused by the combustion of fossil fuels, application of fertilizers, and expansion of $N_2$-fixing crops (Davidson, 2009; Peñuelas et al., 2013; Peñuelas and Sardans, 2022). This imbalance in nutrient stoichiometry threatens terrestrial ecosystems and has received great attention (Peñuelas and Sardans, 2022). Increasing evidence from studies reporting increased N:P ratios in soils and microbial biomass, accompanied by decreased levels of available P and microbial biomass P in the soil caused by N addition, supports the hypothesis that N deposition exacerbates P limitation in terrestrial ecosystems (Deng et al., 2017; Fan et al., 2020; Li et al., 2016; Wang et al., 2023). However, N deposition could partly increase P supply by enhancing plant and microbial phosphatase activity (Chen et al., 2020). These contrasting findings indicate that the response of soil P availability to N deposition remains uncertain, highlighting the necessity to determine the underlying mechanisms of such discrepancies and assess the effects of N deposition on forest ecosystems at the global and regional scales.

Microorganisms play a fundamental role in soil P cycling and regulating P availability in forest ecosystems (Liang et al., 2020; Richardson and Simpson, 2011). Low P availability may considerably affect soil community composition by strengthening the interaction between certern microbial taxa with common habitats and functions, leading to the formation of microbial ecological modules capable of ameliorating P limitation (Fan et al., 2021a). A recent study used co-occurrence network analysis to construct a microbial ecological module and identify the keystone phylotypes that regulate P cycling in agroecosystems under long-term

fertilization (Fan et al., 2021a). Forest ecosystems are more prone to P limitation than agroecosystems because the former lack artificial fertilization, and the weathering of P-containing rocks is the key P source (Reinhard et al., 2017; Walker and Syers, 1976). Microbes play an essential role in P transformation in forest soils (Dai et al., 2020; Liang et al., 2020; Richardson and Simpson, 2011). However, information regarding the dominant ecological module phylotypes and their roles in P transformation remains limited.

Microorganism-mediated soil P transformation is mainly attributed to four microbial gene categories: genes involved in P starvation response regulation (e.g., *phoU* and *phoR*), inorganic P solubilization (e.g., *gcd*), organic P mineralization (e.g., *phoD and phoA*), and P uptake and transport (e.g., *pst and pit*) (Bergkemper et al., 2016; Liang et al., 2020). The *phoR-phoB* two-component regulatory system detects extracellular changes in P concentration and regulates the expression of genes involved in P cycling. Upon encountering P limitation, the expression of the sensor *phoR* activates the response regulator *phoB*, which consequently activates P-starvation response regulation, enabling microorganisms to use alternative P sources (Hsieh and Wanner, 2010; Lubin et al., 2016; Wanner, 1993). Although this paradigm of microbial molecular mechanisms affecting P utilization has been demonstrated in *Escherichia coli in vitro* (Hsieh and Wanner, 2010), further studies are required to determine whether two-component regulatory systems mediate P cycling *in situ* (forest soil).

Microbial functional genes are expected to regulate inorganic P solubilization and organic P mineralization processes in the soil when P availability is limited (Alori et al., 2017; Dai et al., 2020). Liang et al. (2020) reported that the enhanced levels of available P found in mining degraded land after ecological restoration are mainly attributed to the solubilization of

inorganic P driven by enhanced *gcd* gene expression. Another study revealed that N addition increased organic P mineralization because of the upregulation of the *phoD* gene (phosphatase) in microbes (Wang et al., 2018a). Thus, microbes may trigger different functional genes to regulate P availability in soils with varying accessibility to inorganic or organic P. Nevertheless, in subtropical forest soils with a high phosphate sorption capacity (Vitousek and Farrington, 1997), the group of microbial functional genes that is predominantly involved in P transformation to counter the N deposition-induced soil P limitation remains unclear.

Owing to severe weathering and the immobilization of P by iron or aluminum oxides, subtropical forest soils are characterized by low P availability (Walker and Syers, 1976; Zhou et al., 2018). Furthermore, N deposition stimulates plant growth and can further increase P demand (Fan et al., 2018), thereby intensifying the gap between P supply and demand in the soil. Therefore, evaluating soil P availability in response to N deposition and the underlying mechanisms are critical for predicting the productivity of subtropical forest ecosystems. In the present study, Moso bamboo (*Phyllostachys heterocycla cv. Pubescens*), one of the most important non-timber forest plants in the world (Peng et al., 2013), was selected to conduct a simulated N deposition experiment to explore the mechanism of microorganism-driven P cycling in soil. We hypothesized that: 1) N deposition may induce stoichiometric imbalance of soil microbial biomass and thus enhance microbial function in mobilizing soil P; 2) microbes mainly upregulate organic P mineralization rather than inorganic P solubilization genes to alleviate P limitation because organic P is a major P source in subtropical forest soil.

## 2. Material and methods

### *2.1. Site description and sampling*

This study was conducted in the Daiyun Mountain Nature Reserve located in Dehua County, Fujian Province, southeast China (118°05'22"–118°20'15" E, 25°38'07"–25°43'40" N; 1200 m above sea level). This region is characterized by a subtropical humid monsoon climate (Zeng et al., 2022), which can be simultaneously hot and humid, with minimum and maximum average temperatures of 8.5 and 25.5 °C in January and July (30-year average), respectively. The average annual precipitation is 1,800 mm, primarily occurring during the monsoon period (March–September), while the average relative humidity is 80%. The soil in this region is classified as Ultisol according to the USDA Soil Taxonomy. The experimental site consisted of a pure Moso bamboo forest with few trees or shrubs where the bamboo trees were mostly regenerated during 2015–2016.

Nine 3 × 10 m experimental plots were randomly selected in the study area. These plots had similar slopes and elevations and were facing the same direction. Three different levels of N were applied to the plots: control (CT, 0 kg N $ha^{-1}\cdot yr^{-1}$), low N application (LN, 20 kg N $ha^{-1}\cdot yr^{-1}$), and high N application (HN, 80 kg N $ha^{-1}\cdot yr^{-1}$). Each treatment had three replicates, resulting in a total of nine experimental plots. The experiment was initiated in July 2014. For the LN and HN plots, appropriate amounts of $NH_4NO_3$ were dissolved in 20 L of deionized water. The solution was sprayed evenly on these plots monthly during the growing season (March to September). The CT plots received an equivalent volume of deionized water. No other cultivation activities, such as fertilizing with other nutrients, weeding, or felling, were performed during the experimental period.

Leaf sampling was conducted following the methods described previously (Li et al., 2021a). In July 2019, 20 healthy leaves from the mid-upper canopy on the south-facing side of each bamboo plant were collected. These leaves were mixed to create a pooled sample for each plot. Immediately after collection, the leaves were flash-frozen in dry ice and stored at -80 ℃ during transportation to the laboratory. Subsequently, the samples were dried at 105 ℃ for 30 min, followed by incubation at 65 ℃ until a constant weight was achieved. The dried samples were then milled before measuring the P concentration.

For soil sampling, five topsoil cores from a depth of 0 to 15 cm were randomly collected from each of the three replicate plots in July 2017, 2018, and 2019. After removing the litter layer, the soil samples were mixed and homogenized to create a pooled sample for each plot. A total of 27 soil samples were collected, sealed in plastic bags, and transported to the laboratory. The soil samples were sieved (< 2 mm) to remove visible roots and stones. The soil samples were divided into two parts. One part was stored at 4 ℃ for determining microbial characteristics and extracting DNA within two weeks. The other part was air-dried and used for the analysis of available, organic, and total P in the soil, as well as other soil properties. Fine roots (0–2 mm in diameter) of Moso bamboo were carefully cleaned and collected. The root samples were dried at 105 ℃ for 30 min, then dried to a constant weight at 65 ℃. They were then ground and sieved through a 0.149 mm mesh sieve.

*2.2. Soil Chemical Analysis*

Foliar and root P concentrations were evaluated by digesting the samples with $H_2SO_4$ and $HClO_4$ (4:1) (Xu et al., 2017) and measured using a continuous flow analyzer (San++; Skalar,

the Netherlands). Soil pH was measured in a 1:2.5 (w/v) soil-to-water extract using a pH meter (STARTER300; OHAUS, USA). Soil organic C (SOC) and total N (TN) were determined using an elemental analyzer (Elementar Vario EL III; Elementar Analysensysteme GmbH, Germany). The $NH_4^+$-N and $NO_3^-$-N were extracted with 2 mol $L^{-1}$ KCl, and determined using a continuous-flow analytical system (Skalar San++, Breda, the Netherlands) (Carter and Gregorich, 2007). Mineral N (MN) was calculated as the summary of $NH_4^+$-N and $NO_3^-$-N. Soil available P was extracted using 0.5 M $NaHCO_3$ (Watanabe and Olsen, 1965), whereas soil organic P was extracted with 1 M $H_2SO_4$ after ignition at 500 °C for 1 h (Walker et al., 1958). Finally, the total soil P was evaluated using sulfuric acid and perchloric acid digestion. A continuous-flow analytical system was used to determine phosphate concentrations in the soil extract samples. Soil microbial biomass C, N, and P concentrations (MBC, MBN, and MBP, respectively) were measured using the chloroform fumigation–extraction method (Vance et al., 1987). Soil microbial biomass C, N, and P (MBC, MBN, and MBP, respectively) were determined using the chloroform fumigation–extraction method. The conversion factors for MBC, MBN, and MBP were 0.45, 0.54, and 0.40, respectively (Brookes et al., 1982; Li et al., 2021b; Vance et al., 1987). P nitrophenyl phosphate was used as a substrate to assay the potential activities of acid phosphatase (ACP) and alkaline phosphatase (ALP) in a modified universal buffer (pH = 5.0, pH = 11.0) (Saiya-Cork et al., 2002; Zhang et al., 2012). Furthermore, bis-*p*-nitrophenyl phosphate was used as a substrate to assay the potential activity of phosphodiesterase (PD) in a THAM-acetate buffer (pH = 8) (Tian et al., 2021). Phosphatase activity was measured using 365 nm excitation and 450 nm emission filters on a SpectraMax M5 Microplate Reader (MDS Analytical Technologies, Molecular Devices, USA).

*2.3. DNA extraction, PCR amplification, and sequencing*

Soil DNA was extracted using the E.Z.N.A.® soil DNA Kit (Omega Bio-tek, Norcross, GA, USA), according to the manufacturer's instructions. DNA was visualized on 1% agarose gels and measured using a NanoDrop 2000 UV-vis spectrophotometer (Thermo Scientific, Wilmington, USA).

The variable V3-V4 regions of the bacterial 16S rRNA gene were amplified using the primers 338F (ACTCCTACGGGAGGCAGCAG) and 806 R (GGACTACNNGGGTATCTAAT) (Caporaso et al., 2011). For fungi, the ITS1 region of fungal rRNA was amplified using ITS1 (CTTGGTCATTTAGAGGAAGTAA) and ITS2 (TGCGTTCTTCATCGATGC) primer sets (Wang et al., 2022a). PCR analysis was performed in triplicates and consisted of 20 μL reaction mixture containing 4 μL of 5 × FastPfu Buffer, 2 μL of 2.5 mM dNTPs, 0.8 μL of each primer (5 μM), 0.4 μL of FastPfu Polymerase, and 10 ng of DNA template. Sequencing was performed on an Illumina MiSeq platform (Illumina, San Diego, CA, USA), according to the standard protocols provided by Majorbio Bio-Pharm Technology Co., Ltd. (Shanghai, China). Metagenomic sequencing was performed as follow. DNA extract was fragmented to an average size of about 400 bp using Covaris M220 (Gene Company Limited, China) for paired-end library construction. Paired-end library was constructed using NEXTFLEX Rapid DNA-Seq (Bioo Scientific, Austin, TX, USA). Paired-end sequencing was performed on Illumina NovaSeq (Illumina Inc., San Diego, CA, USA) at Majorbio Bio-Pharm Technology Co., Ltd. (Shanghai, China) using NovaSeq 6000 S4 Reagent Kit v1.5 (300 cycles) according to the manufacturer's instructions.

195

196 *2.4. Processing of sequencing data*

197 Raw FASTQ files were quality-filtered by Trimmomatic and merged by FLASH using the
198 following criteria: (i) reads with an average quality score < 20 over a 50 bp sliding window
199 were truncated at any site; (ii) sequences overlapping more than 10 bp were merged according
200 to their overlap with a mismatch of no more than 2 bp; and (iii) sequences of each sample were
201 separated according to barcodes (exactly matching) and primers (allowing 2 nucleotide
202 mismatching), and reads containing ambiguous bases were removed. Operational taxonomic
203 units (OTUs) with ≥ 97% similarity were clustered using UPARSE (version 7.1;
204 http://drive5.com/uparse/; Edgar, 2013). Phylogenetic taxonomy was conducted using the RDP
205 Classifier algorithm (http://rdp.cme.msu.edu/) against the SILVA database (Quast et al., 2013)
206 for bacteria and UNITE database (Nilsson et al., 2019) for fungi, using a 70% confidence
207 threshold. After quality filtering, 1,543,733 and 790,479 high-quality 16S rRNA genes and ITS
208 sequences were obtained, with a minimum of 47,504 and 29,277 sequences per sample,
209 respectively. After clustering at the 97% level, 16S rRNA genes and ITS sequences were
210 grouped into 5,833 and 1,490 OTUs and used for bacterial and fungal community analyses,
211 respectively. Metagenomic data processing including the procedures for quality control, contig
212 assembly, open reading frames prediction, and taxonomic classification and functional
213 annotation of genes can be found in Text S1 for reference in the Supporting information.

214 Bacterial functional profiles were predicted using the PICRUSt2 software
215 (https://github.com/picrust/picrust2/wiki) and KEGG orthology (de Scally et al., 2016;
216 Douglas et al., 2020). A previously reported dataset was selected to evaluate soil microbial

genes involved in P transformation (Bergkemper et al., 2016; Dai et al., 2020; Mcgrath et al., 2013).

### *2.5. Real-time fluorescence quantitative PCR (qPCR)*

qPCR using primers listed in Table S1 was performed to determine the absolute abundance of predominant genes responsible for P starvation response (*phoU* and *phoR*), inorganic P solubilization (*gcd* and *ppx*) (Liang et al., 2020; Zhang et al., 2023), and organic P mineralization (*phoN*, *phoD*, *phnX*, and *appA*) (Long et al., 2018; Lu et al., 2022). The reaction mixtures included 1.0 μL DNA, 10 μL 2 × Taq PCR Master Mix (Allwegene, Beijing, China), and 0.5 μL (10 μM) of the forward and reverse primers. Sterile water was added to the reactions until the mixture volume was fixed to 18 μL. The amplification conditions were as follows: 94 °C for 5 min, 30 cycles at 94 °C for 30 s, 55 °C for 30 s, 72 °C for 30 s. Standard curves were plotted using a 10 × plasmid DNA dilution series containing the target gene.

### *2.6. Statistical analysis*

A repeated measures ANOVA was performed conducted to assess the impact of N addition level, duration, and their interaction on various variables, including soil available P, organic P, microbial characteristics (biomass and phosphatase), and microbial diversity and richness indices. The significance level was set at $p < 0.05$. The normality of residuals and the homogeneity of variance were assessed using the Shapiro–Wilk and Levene's tests, respectively. Furthermore, significant differences between groups ($p < 0.05$) were determined using Duncan's test. Pearson's correlations were used to examine linear relationships between

variables. All statistical analyses were conducted using IBM SPSS Statistics for Windows (version 21.0; IBM Corp., Armonk, NY, USA).

OTUs with relative abundances exceeding 0.01% in bacterial and fungal sequences were selected for constructing a co-occurrence network (Feng et al., 2021). Initial network relationships were inferred according to the Spearman correlation matrix calculated using the "WGCNA" package in R, version 4.1.2 (http://cran.r-project.org/). In the network, each node represents an OTU, and the edges connecting nodes represent the correlations between OTUs. To control for false-positive results, all *p*-values were adjusted for multiple correlations using the Benjamini and Hochberg false discovery rate (FDR) (Benjamini et al., 2006). Strong correlations with Spearman correlation coefficients > 0.60 and FDR-adjusted *p*-values < 0.01 were selected to construct the co-occurrence networks. The network was visualized using Gephi, version 0.9.2 (http://gephi.github.io/). Subsequently, we identified the major microbial modules of strongly correlated OTUs in the co-occurrence network (modularity value > 0.4), assuming the network had a modular structure (Shi et al., 2016). The relative abundance of each module was calculated by averaging the standard relative abundances (z-scores) of all taxa within the module (Delgado-Baquerizo et al., 2018).

We calculated Spearman correlations between soil enzyme activities and the major bacterial and fungal modules. Additionally, we used the multiple regression model (lm function in the "stats" package in R) (Jiao et al., 2020) with variance decomposition analysis (calc.relimp function in the "relaimpo" package in R) (Grömping et al., 2006) to estimate the importance of the differences in major modules in explaining the dissimilarities in the absolute abundance of P cycling genes. Afterward, to identify the statistically significant predictors in

the absolute abundance of P cycling genes, a random forest analysis was used by incorporating all species in keystone modules into the model using the "rfPermute" package (Feng et al., 2021).

Based on known and potential relationships, a structural equation model (SEM) was used to evaluate the direct or indirect effects of microbial P-cycling genes on soil organic P and available P under N addition (Grace, 2006). The SEM was fitted by maximum likelihood estimation using IBM SPSS Amos 21.0 software (Amos Development Corporation, Chicago, IL, USA). The models were considered to have a good fit when the *p*-value > 0.05, standardized root mean square residual (SRMR) < 0.10, and root mean square error of approximation (RMSEA) < 0.08 (Ma et al., 2021). Box plots were generated using the "ggplot2" package in R.

## 3. Results

### *3.1. Foliar and root P concentration*

Five years of N addition significantly increased the aboveground biomass of Moso bamboo (Table S2) and P concentration in the leaves, especially under the HN treatment (Fig. S1; $p < 0.05$). This was also the case for the root P concentration, which significantly increased under N addition treatments during the experimental period ($p < 0.05$).

### *3.2. Soil properties and P status*

N addition did not affect soil pH, SOC, and TN concentrations during the experimental period (Table S3), whereas significantly increased the N availability ($p < 0.05$). N addition also caused

283 a significant decline in available and organic P concentrations in the soil ($p < 0.05$; Figs. 1 and
284 S2), whereas no significant changes were observed in inorganic and total P ($p > 0.05$). Available
285 P and organic P decreased by 32.54% and 27.88%, respectively, in the LN treatment and by
286 5.14% and 24.63%, respectively, in the HN treatment compared with those in the control group.
287
288 *3.3. Microbial biomass C, N, and P*
289 N addition induced a significant reduction in MBP (Table 1; $p < 0.01$); however, it did not affect
290 MBC or MBN ($p > 0.05$). Similarly, N addition did not alter the MBC:MBN ratio but increased
291 the MBC:MBP and MBN:MBP ratios, especially in the $4^{th}$ and $5^{th}$ year of N addition (Table 1).
292
293 *3.4. Phosphatases activities*
294 The activities of ACP ($p < 0.01$) and ALP ($p < 0.05$) were significantly increased by N addition,
295 but not those of PD in the soil ($p > 0.05$; Figs. 2 and S3). The duration of N addition (T) did
296 not affect ACP activity ($p > 0.05$) but significantly increased PD and ALP activities ($p < 0.05$).
297 No significant interactions (T × N) were observed between the N addition duration and level
298 on the activities of the three phosphatases ($p > 0.05$).
299
300 *3.5. P-related microbial functional genes*
301 The results of qPCR revealed that N addition significantly increased the absolute abundance of
302 genes involved in P starvation response regulation (*phoU* and *phoR*) and organic P
303 mineralization (*phoN*, *phoD*, and *appA*) ($p < 0.05$; Figs. 3 and S4). N addition also significantly
304 increased the absolute abundance of *pstS* ($p < 0.05$), but did not changed *pitA*. N addition had

minor or negative effects on the absolute abundance of genes involved in inorganic P solubilization (*ppx* and *gcd*).

To obtain more information, we also detected 38 genes regulating P transformation based on PICRUSt2 software; these genes and their corresponding KO numbers are shown in Table S4 and Fig. S5. Similarly, the results of PICRUSt2 showed that N addition induced significant higher relative abundance of P starvation response regulation and organic P mineralization genes, although overall, it had minor effects on P-uptake and P-transport genes and inorganic P solubilization genes (Fig. S6).

### *3.6. Microbial P cycling ecological module*

To further investigate the microbial functional potential associated with soil P cycling, soil microbial communities were grouped into different modules based on co-occurrence networks. Five microbial modules were created for both bacterial (B_Mod#0–5) and fungal (F_Mod#0–5) communities (Fig. 4a). The bacterial modules included eight phyla (*Firmicutes*, *Proteobacteria*, *Actinobacteria*, *Chloroflexi*, *Acidobacteria*, *Planctomaycetes*, *Gemmatimonadetes*, and *Bacteroides*). In contrast, the fungal modules contained five specific (*Ascomycota*, *Basidiomycota*, *Rozellomycota*, *Mortierellomycota*, and *Mucoromycota*) and one unassigned phylum (Fig. S7).

N addition significantly affected the bacterial modules (B_Mod#0–5) and particularly increased the abundance of B_Mod#0 ($p < 0.05$; Fig. S8). In contrast, no significant changes were observed in the abundance of fungal modules (F_Mod#0–5) in response to N addition ($p > 0.05$; Fig. S8). B_Mod#0 was the microbial module that contributed the most to changes in P

cycle functional genes (> 60%; Fig. 4b), with a significant positive correlation with P starvation response regulation (e.g., *phoU* and *phoR*) and mineralization (e.g., *phoN*, *phoD*, *phnX*, and *appA*) genes ($p < 0.05$; Figs. 4b and S9). *Proteobacteria*, *Firmicutes*, and *Actinobacteria* were the dominant phyla in B_Mod#0, and their relative abundances increased with N addition (Table S5). Moreover, random forest analysis revealed that these taxa were the most important taxonomic phyla responsible for the increase in P mineralization genes abundance (Fig. 4c; Table S5). These findings suggest that the B_Mod#0 act as the keystone modules controlling potential P cycling.

### *3.7. Relationships between soil P status, microbial functional traits and enzyme activities*

SEM was used to explore the direct and indirect pathways by which microorganisms regulated soil P availability under N addition (Fig. 5). Results showed that the MBN:MBP ratio was positively correlated with the absolute abundance of P starvation response regulation genes. The increased expression of P starvation response regulation genes mostly upregulated the expression of P mineralization genes but not P solubilization genes, consequently enhancing the activities of phosphatase, which indirectly accelerated organic P mineralization (Fig. 5).

## 4. Discussion

### *4.1. Soil P status and microbial biomass P in response to N addition*

In this study, a significant decrease in soil P availability induced by N addition was observed (Fig. 1), which is in agreement with studies reporting the effect of N addition on subtropical *Pinus elliottii* plantations and *Castanopsis* forests (Fan et al., 2020; Kou et al., 2018). These

findings support the hypothesis that N deposition exacerbates P limitation in subtropical forest soils with low P availability (Fan et al., 2019a; Li et al., 2016; Vitousek et al., 2010). N addition usually leads to the leaching of exchangeable base cations (e.g., $Ca^{2+}$ and $Mg^{2+}$; Li et al., 2018; Pereg et al., 2018), which may activate Al and hydrous oxides and thereby enhancing phosphate fixation (Fan et al., 2019a; Wang et al., 2022b; Zhou et al., 2018). Another reason is the rapid uptake of P caused by N deposition-stimulated plant growth (Fan et al., 2018; Kimmel et al., 2020; Yang et al., 2019), which was also evident by the fact that the aboveground biomass and P concentrations in Moso bamboo increased after N addition (Table S2 and Fig. S1).

However, organic P concentration declined significantly after N addition (Fig. 1). Similarly, previous studies have reported that organic P decreased because of experimental N enrichment in a subtropical natural forest and deciduous forests in the Bear Brook (Fan et al., 2018; Heuck et al., 2018). Considering that organic P serves as an important source of available P after decomposition (Fan et al., 2021b), its decrease implies that continuous N deposition may deplete potential P sources in subtropical forest soils stored in the form of organic P (Yang et al., 2021). Contrastingly, no significant changes in inorganic P were observed following N addition. One possible reason is that less than 2% of the inorganic P belongs to bioavailable P and can be utilized, while majority of the inorganic P is fixed by Fe and Al oxides and minerals (Carreira et al., 2000; Fan et al., 2019a). Therefore, inorganic P may be inaccessible to microbes and plant roots and insensitive to environmental changes, thereby contributing to the unchanged inorganic P observed. Furthermore, the decomposition of organic P releases inorganic P, which is subsequently absorbed by soil minerals, compensating the loss of inorganic P and maintaining the equilibrium of inorganic P in the soil.

Microbes play a critical role in regulating nutrient cycling in the soil, and soil microbial biomass is sensitive to environmental changes and inputs such as N deposition (Carrara et al., 2021; Li et al., 2014; Moore et al., 2021; Wang et al., 2018b; Zhang et al., 2018). We found that N addition significantly decreased MBP but increased MBC:MBP and MBN:MBP (Table 1). Besides, the results of enzymatic stoichiometry revealed that the vector angle was > 45° and increased with N addition (Fig. S10; unpublished data). These results indicate that additional N input could increase microbial P demand and may even intensify the P limitation for microbes at the study site. This can be further supported by an increase in the ACP and ALP activities (Fig. 2) and an experiment with P addition in vitro (Zeng et al., 2024). Nevertheless, no significant changes in MBC and MBN were observed, despite that N addition directly increased soil N availability (Table S3). It is possible that microbial growth was more limited by P, leading to a greater investment of C and N in acquiring P (e.g., producing phosphatase) rather than storing them in microbial biomass. An alternative or complementary explanation is that N addition did not reduce the pH (Table S3), owing to $Al^{3+}$ serving as the dominant cation in buffering soil acidification when the pH approaches 4.5 (Bowman et al., 2008; Tian and Niu, 2015). The stronger buffering capacity of $Al^{3+}$ compared to that by exchangeable based cations maintains stable pH levels, thereby protecting microbes from the harmful effects induced by a low pH (Vitousek and Farrington, 1997; Zhang et al., 2018).

*4.2. Soil microbial P function potential in response to N addition*

Consistent with the increase in phosphatase activity, N addition significantly enhanced the absolute abundance of P cycling genes, including those involved in P starvation response

393 regulation (e.g., *phoU* and *phoR*) and organic P mineralization (e.g., *phoN*, *phoD*, and *appA*)
394 (Figs. 3, S4, and S5). Previous studies have also found that soil microorganisms upregulate the
395 expression of functional genes harboring phosphatases (e.g., *appA*, *phoN*, *and phoD*) under soil
396 P deficiency conditions (Jiang et al., 2021; Liang et al., 2020; Ragot et al., 2017; Wei et al.,
397 2019). These findings suggest that N deposition stimulates the microbial P starvation response
398 and enhances organic P hydrolysis by microbes (Fan et al., 2018; Heuck et al., 2018).
399 Contrastingly, Dai et al. (2020) reported that N fertilizer increased the abundance of *phoR* but
400 reduced *phoD* in agroecosystem soil, attributed to a decline in pH. This decline suggests an
401 inhibitory effect of soil acidification on microbial-driven organic P mineralization. Therefore,
402 the sustained pH in this study is conducive to microbial functional performance, which offers
403 an explanation for the increased abundance of organic P mineralization genes. Furthermore, N
404 addition significantly increased the abundance of *pstS*, which encodes high-affinity phosphate-
405 specific transporter, but had minor impact on *pitA*, a gene that encodes a transporter with low-
406 affinity. This suggests that in low P soil, microbes prioritize the expression of high-affinity *pstS*
407 over *pitA* to facilitate phosphate transportation (Hsieh and Wanner, 2010).

408 In contrast to the increased abundance of P mineralization genes, the abundance of
409 inorganic P solubilization genes (*gcd* and *ppx*) did not increase after N addition (Fig. 3). This
410 indicates that microbes at the study site utilize P from organic P mineralization rather than
411 inorganic P solubilization again, which is contrary to the earlier studies reporting that inorganic
412 P desorption serves as an important resource of bioavailable P (Ghodszad et al., 2022; Liang et
413 al., 2020). These conflicting results may partly be attributed to the availability of inorganic or
414 organic P and their ease of accessibility by soil microbes. In the experimental plots, due to its

strong adsorption to Fe and Al oxides, most inorganic P was hard to be accessed and utilized by microbes and thus non-bioavailable (Vitousek and Farrington, 1997; Walker and Syers, 1976). Contrastingly, organic P accounts for approximately 40% of soil total P (Fan et al., 2019a; Fan et al., 2021b) and is more easily desorbed from soil oxides and enzymatically hydrolyzed to release available P for microorganisms compared to that by inorganic P (Fan et al., 2018; Landeweert et al., 2001; Richardson and Simpson, 2011). Furthermore, earlier studies focusing on the influence of N deposition on soil P fractions emphasized that organic P is critical in supplying available P to plants and microbes in subtropical areas (Fan et al., 2018; Fan et al., 2019a). This is further supported by the positive correlation between organic P and MBP observed in this study (Fig. S11). Furthermore, we observed that ACP had higher explanation ($R^2$ = 0.54) than that by ALP ($R^2$ = 0.37) for the decrease in organic P (Fig. S12). This result supports the fact that ACP plays a more important role than that by ALP in organic P mineralization in acidic soils, as ACP demonstrates maximal activities in acidic conditions (Tazisong et al., 2015; Zheng et al., 2021). This is further corroborated by the increased expression of the genes *phoN*, which encode ACP, following N addition. Overall, we speculated that microorganisms respond to P deficiency primarily by increasing the abundance of P mineralization genes and the associated organic P decomposition.

*4.3. Keystone microbial ecological modules associated with P transformation under N addition*

To cope with nutrient deficiency (e.g., N and P), soil microbes may reestablish their potential associations and form modules to ameliorate nutrient limitation (Fan et al., 2019b; Fan et al., 2021a; Han et al., 2021). This was confirmed in the present study, revealing that B_Mod# was

437 the keystone module regulating P cycling functional potential. Furthermore, the abundance of
438 some *Proteobacteria*, *Actinobacteria*, and *Firmicutes* in B_Mod#0 increased with N addition
439 and were the key phyla contributing to the increase in organic P mineralization genes
440 abundance (Fig. 4c; Table S5). *Proteobacteria*, *Actinobacteria*, and *Firmicutes* were
441 demonstrated to contain phosphatases encoding genes such as *phoN* (coding for ACP) and
442 *phoD* (coding for ALP) (Alori et al., 2017; Franco-Correa et al., 2010; Ragot et al., 2017; Wei
443 et al., 2016), and their abundance is positively correlated with phosphatase enzyme activity
444 (Cui et al., 2018). These findings indicate that N addition increased the abundances of
445 *Proteobacteria*, *Actinobacteria*, and *Firmicutes* phyla, and strengthened their association to
446 form B_Mod#0, ultimately contributing to activate soil P.

447 To clarify the molecular mechanism of microbial-driven P mineralization, we further
448 identified the keystone taxa in the present study. Our analysis revealed that the
449 *Alphaproteobacteria* of *Proteobacteria* phylum covered most *phoD* and *phoN*-harboring
450 bacteria, and were significantly increased after N addition (Fig. S13). Such findings implied
451 that the N input increased *Alphaproteobacteria*, enhancing expression of P-mineralization
452 genes, which subsequently regulated the production of P-cycling enzymes (e.g., ACP and ALP)
453 and thus contributed to soil P transformation in the experimental plot.

454

455 *4.4. Pathway of soil microorganisms involved in enzymatic hydrolysis of organic P under N*
456 *application*

457 In this study, we identified the key modules and phyla of soil microorganisms involved in
458 organic P decomposition (Fig. 4). However, the mechanism by which N deposition triggers

these processes remains unclear. SEM analysis revealed that N addition led to an imbalance in soil nutrient stoichiometry and intense P deficiency, as evidenced by the increased MBN:MBP ratio and decrease in soil P availability. In response to environmental P shortages, soil microbes effectively assimilate alternative forms of P from the soil by activating the *phoR*/*phoB* two-component signal transduction system (Eder et al., 1996; Hsieh and Wanner, 2010; Lubin et al., 2016). For example, under P limitation, *E. coli* upregulates the *phoR* sensor, which phosphorylates the response regulator *phoB* and activates the phosphate regulon. However, under excessive P conditions, *phoR, pstS, and phoU* dephosphorylate *phoB* and deactivate the phosphate regulons (Hsieh and Wanner, 2010; Wanner, 1993). Similarly, our study found that N addition enhanced the absolute abundance of P starvation response regulation genes, suggesting that the two-component signaling system might regulate the expression of P starvation response genes in microbes under P limitation conditions in the forest soil.

Furthermore, we found that an increase in the absolute abundance of P starvation response genes (path coefficient = 0.91) had a positive effect on organic P mineralization genes (e.g., *phoN and phoD*) (Fig. 5). These results are consistent with the findings of a previous study, in which the expression of the P mineralization gene *phoD* was dependent on the sensor gene *phoR* (Eder et al., 1996), suggesting that the enhanced expression of organic P mineralization genes might be a result of the activation of P starvation response genes because of N application. Microorganisms secrete extracellular enzymes, such as ACP and ALP, as products of the corresponding encoding genes, *phoN* and *phoD* genes, respectively (Eder et al., 1996; Liang et al., 2020; Luo et al., 2017; Ragot et al., 2017). Therefore, the increased abundance of the organic P-mineralization genes under N application might enhance microbial phosphatase

481 production (Eder et al., 1996). These results could support the causal relationship between
482 organic P mineralization genes (*phoN and phoD*) and phosphatase activities (ACP and ALP)
483 (Fig. 5).

484 Furthermore, the SEM results showed that phosphatase activity was negatively correlated
485 with organic P (Fig. 5), consistent with the results of previous studies that showed that higher
486 phosphatase activity facilitates organic P hydrolysis (Fujita et al., 2017; Sharma et al., 2020).
487 Thus, the decomposition of organic P resulted in the release of available P. Collectively, our
488 findings suggest that microbial-driven P transformation plays a critical role in meeting
489 increased P demand of Moso bamboo, a rapid-growing species with well-developed
490 underground root system. This, in turn, induces an intense microbial P "starvation response",
491 thereby driving soil P-cycling (Fig. 6). However, the suitability of such mechanisms for driving
492 organic P mineralization in other forest soils still requires further field-based evidence,
493 especially in tropical and subtropical forests with high species diversity.

494

495 **5. Conclusion**

496 In this study, we observed that N addition exacerbated microbial P limitation, as indicated by
497 imbalanced nutrient stoichiometry (MBC:MBP and MBN:MBP) and significantly decreased
498 soil available and organic P. To cope with P limitations, microorganisms formed microbial
499 modules, with *Proteobacteria*, *Actinobacteria*, and *Firmicutes* being the predominant bacterial
500 phyla in the functional module (B_Mod#0). These bacterial phyla acted as keystone phylotypes,
501 regulating the potential for P cycling. Bacteria harboring P starvation response genes (*phoU*
502 and *phoR*) responded to P deficiency by increasing the absolute abundance of organic P

mineralization genes (*phoN and phoD*), thereby enhancing the hydrolysis of organic P. Our findings provide insights into the molecular mechanisms underlying microbe-driven P cycling in subtropical forest soils under N deposition, specifically in the enzymatic hydrolysis of organic P.

**Acknowledgement**

This research was supported by the National Natural Science Foundation of China (Nos. 41977090, 32192433, and 31922052).

**References**

Alori, E.T., Glick, B.R., Babalola, O.O., 2017. Microbial phosphorus solubilization and its potential for use in sustainable agriculture. Frontiers in Microbiology 8, 971.

Benjamini, Y., Krieger, A.M., Yekutieli, D., 2006. Adaptive linear step-up procedures that control the false discovery rate. Biometrika 93, 491–507.

Bergkemper, F., Scholer, A., Engel, M., Lang, F., Kruger, J., Schloter, M., Schulz, S., 2016. Phosphorus depletion in forest soils shapes bacterial communities towards phosphorus recycling systems. Environmental Microbiology 18, 1988–2000.

Bowman, W.D., Cleveland, C.C., Halada, L., Hreško, J., Baron, J.S., 2008. Negative impact of nitrogen deposition on soil buffering capacity. Nature Geoscience 1, 767–770.

Brookes, P.C., Powlson, D.S., Jenkinson, D.S., 1982. Measurement of microbial biomass phosphorus in soil. Soil Biology and Biochemistry 14, 319–329.

Caporaso, J.G., Lauber, C.L., Walters, W.A., Berg-Lyons, D., Lozupone, C.A., Turnbaugh, P.J., Fierer, N., Knight, R., 2011. Global patterns of 16S rRNA diversity at a depth of millions

526 of sequences per sample. Proceedings of the National Academy of Sciences 108, 4516–
527 4522.
528 Carrara, J.E., Walter, C.A., Freedman, Z.B., Hostetler, A.N., Hawkins, J.S., Fernandez, I.J.,
529 Brzostek, E.R., 2021. Differences in microbial community response to nitrogen
530 fertilization result in unique enzyme shifts between arbuscular and ectomycorrhizal-
531 dominated soils. Global Change Biology 27, 2049–2060.
532 Carreira,J.A., García-Ruiz, R., Liétor, J., Harrison, A.F., 2000. Changes in soil phosphatase
533 activity and P transformation rates induced by application of N- and S-containing acid-
534 mist to a forest canopy. Soil Biology and Biochemistry 32, 1857−1865.
535 Carter, M., Gregorich, E., 2007. Soil sampling and methods of analysis. Soil Sampling and
536 Methods of Analysis. Second ed. CRC Press, Boca Raton, USA.
537 Chen, J., van Groenigen, K.J., Hungate, B.A., Terrer, C., van Groenigen, J.W., Maestre, F.T.,
538 Ying, S.C., Luo, Y., Jørgensen, U., Sinsabaugh, R.L., Olesen, J.E., Elsgaard, L., 2020.
539 Long-term nitrogen loading alleviates phosphorus limitation in terrestrial ecosystems.
540 Global Change Biology 26, 5077–5086.
541 Cui, Y., Fang, L., Guo, X., Wang, X., Wang, Y., Zhang, Y., Zhang, X., 2018. Responses of soil
542 bacterial communities, enzyme activities, and nutrients to agricultural-to-natural
543 ecosystem conversion in the Loess Plateau, China. Journal of Soils and Sediments 19,
544 1427–1440.
545 Dai, Z., Liu, G., Chen, H., Chen, C., Wang, J., Ai, S., Wei, D., Li, D., Ma, B., Tang, C., Brookes,
546 P. C., Xu, J., 2020. Long-term nutrient inputs shift soil microbial functional profiles of
547 phosphorus cycling in diverse agroecosystems. The ISME Journal 14, 757–770.

548 Davidson, E.A., 2009. The contribution of manure and fertilizer nitrogen to atmospheric nitrous
549 oxide since 1860. Nature Geoscience 2, 659–662.
550 de Scally, S.Z., Makhalanyane, T.P., Frossard, A., Hogg, I.D., Cowan, D.A., 2016. Antarctic
551 microbial communities are functionally redundant, adapted and resistant to short term
552 temperature perturbations. Soil Biology and Biochemistry 103, 160–170.
553 Delgado-Baquerizo, M., Reith, F., Dennis, P.G., Hamonts, K., Powell, J.R., Young, A., Singh,
554 B.K., Bissett, A., 2018. Ecological drivers of soil microbial diversity and soil biological
555 networks in the Southern Hemisphere. Ecology 99, 583–96.
556 Deng, Q., Hui, D., Dennis, S., Reddy, K.C., 2017. Responses of terrestrial ecosystem
557 phosphorus cycling to nitrogen addition: A meta-analysis. Global Ecology and
558 Biogeography 26, 713–728.
559 Douglas, G.M., Maffei, V.J., Zaneveld, J.R., Yurgel, S.N., Brown, J.R., Taylor, C.M.,
560 Huttenhower, C., Langille, M.G.I., 2020. PICRUSt2 for prediction of metagenome
561 functions. Nature Biotechnology 38, 685–688.
562 Eder, S., Shi, L., Jensen, K., Yamane, K., Hulett, F.M., 1996. A Bacillus subtilis secreted
563 phosphodiesterase/alkaline phosphatase is the product of a Pho regulon gene, *phoD*.
564 Microbiology 142, 2041–2047.
565 Edgar, R.C., 2013. UPARSE: highly accurate OTU sequences from microbial amplicon reads.
566 Nature Methods 10, 996–998.
567 Fan, K., Delgado-Baquerizo, M., Guo, X., Wang, D., Wu, Y., Zhu, M., Yu, W., Yao, H., Zhu,
568 Y., Chu, H. 2019b. Suppressed N fixation and diazotrophs after four decades of
569 fertilization. Microbiome 7, 143.

570 Fan, K., Delgado-Baquerizo, M., Guo, X., Wang, D., Zhu, Y., Chu, H., 2021a. Biodiversity of
571 key-stone phylotypes determines crop production in a 4-decade fertilization experiment.
572 The ISME Journal 15, 550–561.
573 Fan, Y., Lin, F., Yang, L., Zhong, X., Wang, M., Zhou, J., Chen, Y., Yang, Y., 2018. Decreased
574 soil organic P fraction associated with ectomycorrhizal fungal activity to meet increased
575 P demand under N application in a subtropical forest ecosystem. Biology and Fertility of
576 Soils 54, 149–161.
577 Fan, Y., Lu, S., He, M., Yang, L., Hu, W., Yang, Z., Liu, X., Hui, D., Guo, J., Yang, Y., 2021b.
578 Long-term throughfall exclusion decreases soil organic phosphorus associated with
579 reduced plant roots and soil microbial biomass in a subtropical forest. Geoderma 404,
580 115309.
581 Fan, Y., Yang, L., Zhong, X., Yang, Z., Lin, Y., Guo, J., Chen, G., Yang, Y., 2020. N addition
582 increased microbial residual carbon by altering soil P availability and microbial
583 composition in a subtropical *Castanopsis* forest. Geoderma 375, 114470.
584 Fan, Y., Zhong, X., Lin, F., Liu, C., Yang, L., Wang, M., Chen, G., Chen, Y., Yang, Y., 2019a.
585 Responses of soil phosphorus fractions after nitrogen addition in a subtropical forest
586 ecosystem: Insights from decreased Fe and Al oxides and increased plant roots. Geoderma
587 337, 246–255.
588 Feng, J., Zeng, X., Zhang, Q., Zhou, X., Liu, Y., Huang, Q., 2021. Soil microbial trait-based
589 strategies drive metabolic efficiency along an altitude gradient. ISME Communication 1,
590 1–9.
591 Franco-Correa, M., Quintana, A., Duque, C., Suarez, C., Rodríguez, M.X., Barea, J.M., 2010.

592 Evaluation of actinomycete strains for key traits related with plant growth promotion and
593 mycorrhiza helping activities. Applied Soil Ecology 45, 209–217.
594 Fujita, K., Kunito, T., Moro, H., Toda, H., Otsuka, S., Nagaoka, K., 2017. Microbial resource
595 allocation for phosphatase synthesis reflects the availability of inorganic phosphorus
596 across various soils. Biogeochemistry 136, 325–339.
597 Ghodszad, L., Reyhanitabar, A., Oustan, S., Alidokht, L.J.S., Research, T., 2022. Phosphorus
598 sorption and desorption characteristics of soils as affected by biochar. Soil and Tillage
599 Research 216, 105251.
600 Grace J.B., 2006. Structural Equation Modeling and Natural Systems. Cambridge University
601 Press, Cambridge.
602 Grömping, U., 2006. Relative importance for linear regression in R: the package relaimpo.
603 Journal of Statistical Software 17, 1–27.
604 Han, B., Li, J., Liu, K., Zhang, H., Wei, X., Shao, X., 2021. Variations in soil properties rather
605 than functional gene abundances dominate soil phosphorus dynamics under short-term
606 nitrogen input. Plant and Soil 469, 227–241.
607 Heuck, C., Smolka, G., Whalen, E.D., Frey, S., Gundersen, P., Moldan, F., Fernandez, I.J.,
608 Spohn, M., 2018. Effects of long-term nitrogen addition on phosphorus cycling in organic
609 soil horizons of temperate forests. Biogeochemistry 141, 167–181.
610 Hsieh, Y.J., Wanner, B.L., 2010. Global regulation by the seven-component Pi signaling system.
611 Current Opinion in Microbiology 13, 198–203.
612 Jiang, Z., Zhang, B., Sun, H., Zhang, T., Yu, L., Zhang, Y., 2021. Properties of Modestobacter
613 deserti sp. nov., a Kind of Novel Phosphate-Solubilizing Actinobacteria Inhabited in the

614 Desert Biological Soil Crusts. Frontiers in Microbiology 12, 742798.
615 Jiao, S., Yang, Y., Xu, Y., Zhang, J., Liu, Y., 2020. Balance between community assembly
616 processes mediates species coexistence in agricultural soil microbiomes across eastern
617 China. The ISME Journal 14, 202–216.
618 Kimmel, K., Furey, G.N., Hobbie, S.E., Isbell, F., Tilman, D., Reich, P.B., 2020. Diversity-
619 dependent soil acidification under nitrogen enrichment constrains biomass productivity.
620 Global Change Biology 26, 6594–6603.
621 Kou, L., Jiang, L., Fu, X., Dai, X., Wang, H., Li, S., 2018. Nitrogen deposition increases root
622 production and turnover but slows root decomposition in *Pinus elliottii* plantations. New
623 Phytologist 218, 1450–1461.
624 Landeweert, R., Hoffland, E., Finlay, R.D., Kuyper, T.W., van Breemen, N., 2001. Linking
625 plants to rocks: ectomycorrhizal fungi mobilize nutrients from minerals. Trends in
626 Ecology and Evolution 16, 248–254.
627 Li, J., Li, Z., Wang, F., Zou, B., Chen, Y., Zhao, J., Mo, Q., Li, Y., Li, X., Xia, H., 2014. Effects
628 of nitrogen and phosphorus addition on soil microbial community in a secondary tropical
629 forest of China. Biology and Fertility of Soils 51, 207–215.
630 Li, J., Sang, C., Yang, J., Qu, L., Xia, Z., Sun, H., Jiang, P., Wang, X., He, H., Wang, C., 2021b.
631 Stoichiometric imbalance and microbial community regulate microbial elements use
632 efficiencies under nitrogen addition. Soil Biology and Biochemistry 156, 108207.
633 Li, Q., Lv, J., Peng, C., Xiang, W., Xiao, W., Song, X., 2021a. Nitrogen-addition accelerates
634 phosphorus cycling and changes phosphorus use strategy in a subtropical Moso bamboo
635 forest. Environmental Research Letters 16, 024023.

Li, Y., Niu, S., Yu, G., 2016. Aggravated phosphorus limitation on biomass production under increasing nitrogen loading: a meta-analysis. Global Change Biology 22, 934–943.

Li, Y., Sun, J., Tian, D., Wang, J., Ha, D., Qu, Y., Jing, G., Niu, S., 2018. Soil acid cations induced reduction in soil respiration under nitrogen enrichment and soil acidification. Science of the Total Environment 615, 1535–1546.

Liang, J.L., Liu, J., Jia, P., Yang, T.T., Zeng, Q.W., Zhang, S.C., Liao, B., Shu, W.S., Li, J.T., 2020. Novel phosphate-solubilizing bacteria enhance soil phosphorus cycling following ecological restoration of land degraded by mining. The ISME Journal 14, 1600–1613.

Long, X.E., Yao, H., Huang, Y., Wei, W., Zhu, Y.G., 2018. Phosphate levels influence the utilisation of rice rhizodeposition carbon and the phosphate-solubilising microbial community in a paddy soil. Soil Biology and Biochemistry 118, 103–114.

Lubin, E.A., Henry, J.T., Fiebig, A., Crosson, S., Laub, M.T., 2016. Identification of the PhoB regulon and role of PhoU in the phosphate starvation response of *Caulobacter crescentus*. Journal of Bacteriology 198, 187–200.

Lu, J., Jia, P., Feng, S., Wang, Y., Zheng, J., Ou, S., Wu, Z., Liao, B., Shu, W., Liang, J., Li, J., 2022. Remarkable effects of microbial factors on soil phosphorus bioavailability: A country-scale study. Global Change Biology 28, 4459–4471.

Luo, G., Ling, N., Nannipieri, P., Chen, H., Raza, W., Wang, M., Guo, S., Shen, Q., 2017. Long-term fertilisation regimes affect the composition of the alkaline phosphomonoesterase encoding microbial community of a vertisol and its derivative soil fractions. Biology and Fertility of Soils 53, 375–388.

Ma, S., Chen, G., Tang, W., Xing, A., Chen, X., Xiao, W., Zhou, L., Zhu, J., Li, Y., Zhu, B., Fang, J., 2021. Inconsistent responses of soil microbial community structure and enzyme activity to nitrogen and phosphorus additions in two tropical forests. Plant and Soil 460, 453–468.

McGrath, J.W., Chin, J.P., Quinn, J.P., 2013. Organophosphonates revealed: new insights into the microbial metabolism of ancient molecules. Nature Reviews Microbiology 11, 412–419.

Moore, J.A.M., Anthony, M.A., Pec, G.J., Trocha, L.K., Trzebny, A., Geyer, K.M., van Diepen, L.T.A., Frey, S.D., 2021. Fungal community structure and function shifts with atmospheric nitrogen deposition. Global Change Biology 27, 1349–1364.

Nilsson, R.H., Larsson, K.H., Taylor, A.F.S., Bengtsson-Palme, J., Jeppesen, T.S., Schigel, D., Kennedy, P., Picard, K., Glöckner, F.O., Tedersoo, L., Saar, I., Kõljalg, U., Abarenkov, K., 2019. The UNITE database for molecular identification of fungi: handling dark taxa and parallel taxonomic classifications. Nucleic Acids Research 47, D259–D264.

Peng, Z., L, Y., Li, L., Zhao, Q., Feng, Q., Gao, Z., Lu, H., Hu, T., Yao, N., Liu, K., Li, Y., Fan, D., Guo, Y., Li, W., Lu, Y., Weng, Q., Zhou, C., Zhang, L., Huang, T., Zhao, Y., Zhu, C., Liu, X., Yang, X., Wang, T., Miao, K., Zhuang, C., Cao, X., Tang, W., Liu, G., Liu, Y., Chen, J., Liu, Z., Yuan, L., Liu, Z., Huang, X., Lu, T., Fei, B., Ning, Z., Han, B., Jiang, Z., 2013. The draft genome of the fast-growing non-timber forest species moso bamboo (*Phyllostachys heterocycla*). Nature Genetics 45, 456–461.

Peñuelas, J., Poulter, B., Sardans, J., Ciais, P., van der Velde, M., Bopp, L., Boucher, O., Godderis, Y., Hinsinger, P., Llusia, J., Nardin, E., Vicca, S., Obersteiner, M., Janssens, I.A.,

2013. Human-induced nitrogen-phosphorus imbalances alter natural and managed ecosystems across the globe. Nature Communications 4, 2934.

Peñuelas, J., Sardans, J.J.S., 2022. The global nitrogen-phosphorus imbalance. Science 375, 266–267.

Pereg, L., Morugán-Coronado, A., McMillan, M., García-Orenes, F., 2018. Restoration of nitrogen cycling community in grapevine soil by a decade of organic fertilization. Soil and Tillage Research 179, 11–19.

Quast, C., Pruesse, E., Yilmaz, P., Gerken, J., Schweer, T., Yarza, P., Peplies, J., Glöckner, F.O., 2013. The SILVA ribosomal RNA gene database project: improved data processing and web-based tools. Nucleic Acids Research 41, D590–D596.

Ragot, S.A., Kertesz, M.A., Mészáros, É., Frossard, E., Bünemann, E.K., 2017. Soil *phoD* and *phoX* alkaline phosphatase gene diversity responds to multiple environmental factors. FEMS Microbiology Ecology 93, fiw212.

Reinhard, C.T., Planavsky, N.J., Gill, B.C., Ozaki, K., Robbins, L.J., Lyons, T.W., Fischer, W.W., Wang, C., Cole, D.B., Konhauser, K.O., 2017. Evolution of the global phosphorus cycle. Nature 541, 386–389.

Richardson, A.E., Simpson, R.J., 2011. Soil microorganisms mediating phosphorus availability update on microbial phosphorus. Plant physiology 156, 989–996.

Sharma, S., Compant, S., Ballhausen, M.B., Ruppel, S., Franken, P., 2020. The interaction between *Rhizoglomus irregulare* and hyphae attached phosphate solubilizing bacteria increases plant biomass of *Solanum lycopersicum*. Microbiological Research 240, 126556.

Shi, S., Nuccio, E.E., Shi, Z.J., He, Z., Zhou, J., Firestone, M.K., 2016. The interconnected rhizosphere: high network complexity dominates rhizosphere assemblages. Ecology letters 19, 926–936.

Saiya-Cork, K.R., Sinsabaugh, R.L., Zak, D.R., 2002. The effects of long term nitrogen deposition on extracellular enzyme activity in an Acer saccharum forest soil. Soil Biology and Biochemistry 34, 1309–1315

Tazisong, I.A., Senwo, Z.N., He, Z., 2015. Phosphatase hydrolysis of organic phosphorus compounds. Advances in Enzyme Research 3, 39–51.

Tian, D., Niu, S., 2015. A global analysis of soil acidification caused by nitrogen addition. Environmental Research Letters 10, 024019.

Tian, J., Kuang, X., Tang, M., Chen, X., Huang, F., Cai, Y., Cai, K., 2021. Biochar application under low phosphorus input promotes soil organic phosphorus mineralization by shifting bacterial *phoD* gene community composition. Science of the Total Environment 779, 146556.

Vance, E.D., Brookes, P.C., Jenkinson, D.S., 1987. An extraction method for measuring soil microbial biomass C. Soil Biology and Biochemistry 19, 703–707.

Vitousek, P.M., Farrington, H., 1997. Nutrient limitation and soil development: experimental test of a biogeochemical theory. Biogeochemistry 37, 63–75.

Vitousek, P.M., Porder, S., Houlton, B.Z., Chadwick, O.A., 2010. Terrestrial phosphorus limitation: mechanisms, implications, and nitrogen—phosphorus interactions. Ecological Applications 20, 5–15.

Walker, T., Syers, J.K., 1976. The fate of phosphorus during pedogenesis. Geoderma 15, 1–19.

722 Walker, T.W., Adams, A.F.R., 1958. Studies on soil organic matter: I. Influence of phosphorus
723 content of parent materials on accumulations of carbon, nitrogen, sulfur, and organic
724 phosphorus in grassland soils. Soil Science 85, 307–318.
725 Wang, C., Liu, D., Bai, E., 2018b. Decreasing soil microbial diversity is associated with
726 decreasing microbial biomass under nitrogen addition. Soil Biology and Biochemistry 120,
727 126–133.
728 Wang, R., Yang, J., Liu, H., 2022b. Nitrogen enrichment buffers phosphorus limitation by
729 mobilizing mineral-bound soil phosphorus in grasslands. Ecology 103, e3616.
730 Wang, S., Xiao, J., Wan, L., Zhou, Z., Wang, Z., Song, C., Zhou, Y., Cao, X., 2018a. Mutual
731 dependence of nitrogen and phosphorus as key nutrient elements: one facilitates
732 Dolichospermum flos-aquae to overcome the limitations of the other. Environmental
733 Science and Technology 52, 5653–5661.
734 Wang, X., Sheng, L., Li, Y., Jiang, H., Lv, Z., Qi, W., Luo, W., 2022a. Soil labile organic carbon
735 indicating seasonal dynamics of soil organic carbon in northeast peatland. Ecological
736 Indicators 138, 108847.
737 Wang, X., Li, S., Zhu, B., Homyak, P.M., Chen, G., Yao, X., Wu, D., Yang, Z., Lyu, M., Yang,
738 Y., 2023. Long-term nitrogen deposition inhibits soil priming effects by enhancing
739 phosphorus limitation in a subtropical forest. Global Change Biology 29, 4081–4093.
740 Wanner, B.J., 1993. Gene regulation by phosphate in enteric bacteria. Journal of Cellular
741 Biochemistry 51, 47–54.

742 Watanabe, F., Olsen, S., 1965. Test of an ascorbic acid method for determining phosphorus in
743 water and $NaHCO_3$ extracts from soil. Soil Science Society of America Journal 29, 677–
744 678.
745 Wei, X., Hu, Y., Razavi, B.S., Zhou, J., Shen, J., Nannipieri, P., Wu, J., Ge, T., 2019. Rare taxa
746 of alkaline phosphomonoesterase-harboring microorganisms mediate soil phosphorus
747 mineralization. Soil Biology and Biochemistry 131, 62–70.
748 Wei, Y., Wei, Z., Cao, Z., Zhao, Y., Zhao, X., Lu, Q., Wang, X., Zhang, X., 2016. A regulating
749 method for the distribution of phosphorus fractions based on environmental parameters
750 related to the key phosphate-solubilizing bacteria during composting. Bioresource
751 Technology 211, 610–617.
752 Xu, Z., Yu, G., Zhang, X., He, N., Wang, Q., Wang, S., Wang, R., Zhao, N., Jia, Y., Wang, C.,
753 2017. Soil enzyme activity and stoichiometry in forest ecosystems along the North-South
754 Transect in eastern China (NSTEC). Soil Biology and Biochemistry 104, 152–163.
755 Yang, L., Yang, Z., Peng, Y., Lin, Y., Xiong, D., Li, Y., Yang, Y., 2019. Evaluating P availability
756 influenced by warming and N deposition in a subtropical forest soil: a bioassay mesocosm
757 experiment. Plant and Soil 444, 87–99.
758 Yang, L., Yang, Z., Zhong, X., Xu, C., Lin, Y., Fan, Y., Wang, M., Chen, G., Yang, Y., 2021.
759 Decreases in soil P availability are associated with soil organic P declines following forest
760 conversion in subtropical China. Catena 205, 105459.
761 Zeng, Q., Fan, Y., Zhang, Q., Yuan, X., Lin, K., Zhou, J., Lin, H., Xie, H., Cui, J., Wu, Y., Chen
762 Y., 2022. Differential factors determine the response of soil P fractions to N deposition in
763 wet and dry seasons in a subtropical Moso bamboo forest. Plant and Soil 1–19.

764 Zeng, Q., Liu, Y., Zhang, Q., Mei, K., Yuan, X., Lin, K., Zhou, J., Wu, Y., Xu, M., Chen, Y.,
765 2024. Contrasting priming effect intensities and drivers in single and repeated glucose
766 additions to a forest soil receiving long-term N fertilization. Biology and Fertility of Soils
767 60, 53–58.
768 Zhang, A., Chen, Z., Zhang, G., Chen, L., Wu, J., 2012. Soil phosphorus composition
769 determined by $^{31}$P NMR spectroscopy and relative phosphatase activities influenced by
770 land use. European Journal of Soil Biology 52, 73–77.
771 Zhang, T., Chen, H.Y.H., Ruan, H., 2018. Global negative effects of nitrogen deposition on soil
772 microbes. The ISME Journal 12, 1817–1825.
773 Zhang, Y., Gao, W., Ma, L., Luan, H., Tang, J., Li, R., Li, M., Huang, S., Wang, L., 2023. Long-
774 term partial substitution of chemical fertilizer by organic amendments influences soil
775 microbial functional diversity of phosphorus cycling and improves phosphorus
776 availability in greenhouse vegetable production. Agriculture, Ecosystems and
777 Environment 341, 108193.
778 Zheng, M.M., Wang, C., Li, W.X., Guo, L., Cai, Z.J., Wang, B.R., Chen, J., Shen, R.F., 2021.
779 Changes of acid and alkaline phosphatase activities in long-term chemical fertilization are
780 driven by the similar soil properties and associated microbial community composition in
781 acidic soil. European Journal of Soil Biology 104, 103312.
782 Zhou, K., Lu, X., Mori, T., Mao, Q., Wang, C., Zheng, M., Mo, H., Hou, E., Mo, J., 2018.
783 Effects of long-term nitrogen deposition on phosphorus leaching dynamics in a mature
784 tropical forest. Biogeochemistry 138, 215–224.
785

## Figures legends

**Fig. 1.** Variations in soil available, organic, and total P concentrations after N addition. Box plots show the median (black line), 25 and 75% (box edge), and 10 and 90% of the data set (error bars). T, time effect; N, N addition effect; T × N, interactive effect of time and N addition. ** indicate a significant difference at $p < 0.01$ level. n.s., no significance ($p > 0.05$). Different lowercase letters indicate significant differences between treatments ($n = 9$).

**Fig. 2.** Variations in soil phosphatase activities after N addition. ACP, acid phosphatase; PD, phosphodiesterase; ALP, alkaline phosphatase. Box plots show the median (black line), 25 and 75% (box edge), and 10 and 90% of the data set (error bars). T, time effect; N, N addition effect; T × N, interactive effect of time and N addition. Asterisks (*) indicate a significant difference (*$p < 0.05$, ** $p < 0.01$). n.s., no significance ($p > 0.05$). Different lowercase letters indicate significant differences between treatments ($n = 9$).

**Fig. 3.** Abundance of genes responsible for P starvation response regulation (*phoU* and *phoR*), organic P mineralization (*phoN*, *phoD*, *phnX*, *appA*), inorganic P solubilization (*ppx* and *gcd*), and P-uptake and P-transport (*pitA* and *pstS*). Box plots show the median (black line), 25 and 75% (box edge), and 10 and 90% of the data set (error bars). T, time effect; N, N addition effect; T × N, interactive effect of time and N addition. Asterisks (*) indicate a significant difference (*$p < 0.05$, ** $p < 0.01$, and *** $p < 0.001$). n.s., no significance ($p > 0.05$). Different lowercase letters indicate significant differences between treatments ($n = 9$).

**Fig. 4.** (a) Major bacterial and fungal modules, (b) correlations between modules and P cycling genes, and (c) predominant bacterial phyla (top 10) that influence P cycling genes. (a) Representation of microbial modules induced by N addition. The network diagram nodes represent OTUs colored by each of the major modules within co-occurrence network of bacterial and fungal communities, respectively; (b) identifying the key modules that predominantly contributed to the changes of the abundance of P cycling genes based on correlation and multiple regression models. The size of the circle represents the importance of the variable (i.e., proportion of explained variability calculated via multiple regression modeling and variance decomposition analysis). Colors represent Spearman correlations; (c) the keystone species of key bacterial module (B_Mod#0), responsible for the changes of the abundance of P cycling genes based on random forest analysis. Grey bars indicate species that had no significant effect on the abundance of P cycle genes ($p > 0.05$). Asterisks (*) indicate a significant difference (*$p < 0.05$, ** $p < 0.01$, and *** $p < 0.001$).

**Fig. 5.** Pathway by which soil microorganisms involved in enzymatic hydrolysis of organic P combat soil P deficiency under N addition, revealed by structural equation models (SEM). Red, blue, and grey solid arrows indicate significant positive, negative, and non-significant effects, respectively. * $p < 0.05$, ** $p < 0.01$, and *** $p < 0.001$. MBN:MBP, the ratio of microbial biomass N to microbial biomass P; Phosphatase, represents the summary activities of acid and alkaline phosphatases. GFI, goodness-of-fit index; RMSEA, root mean square error of approximation; SRMR, standardized root mean square residual.

**Fig. 6.** Conceptual framework of enzymatic hydrolysis of organic P co-regulated by keystone bacterial functional module and genes responsible for P mineralization induced by N addition in a subtropical bamboo forest ecosystem.

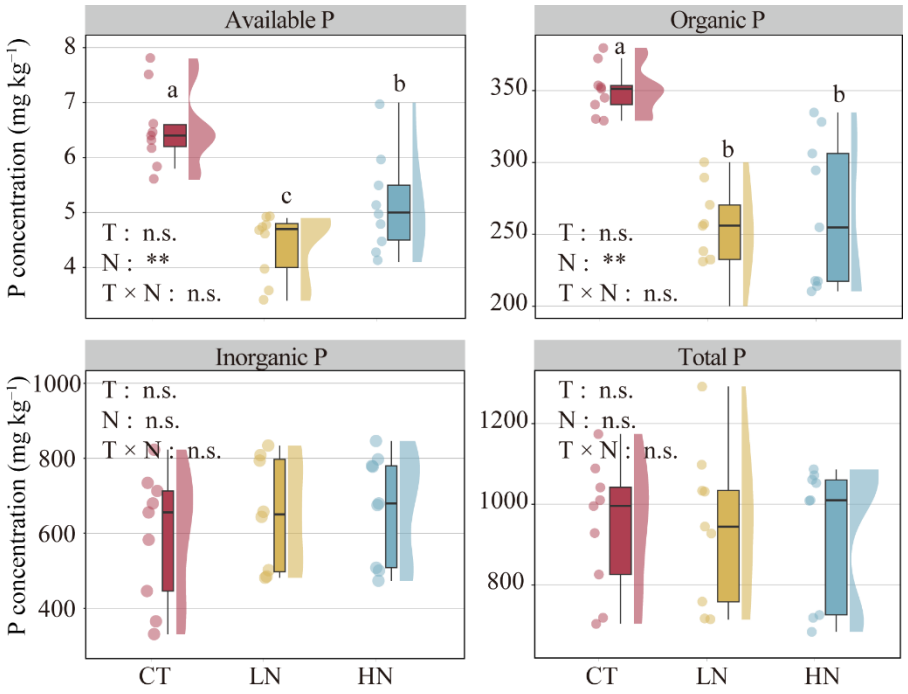
Available P
Organic P
Inorganic P
Total P
P concentration (mg kg⁻¹)
T : n.s.
N : **
T × N : n.s.
T : n.s.
N : n.s.
T × N : n.s.
a
b
c
CT
LN
HN

834

835 **Fig. 1**

836

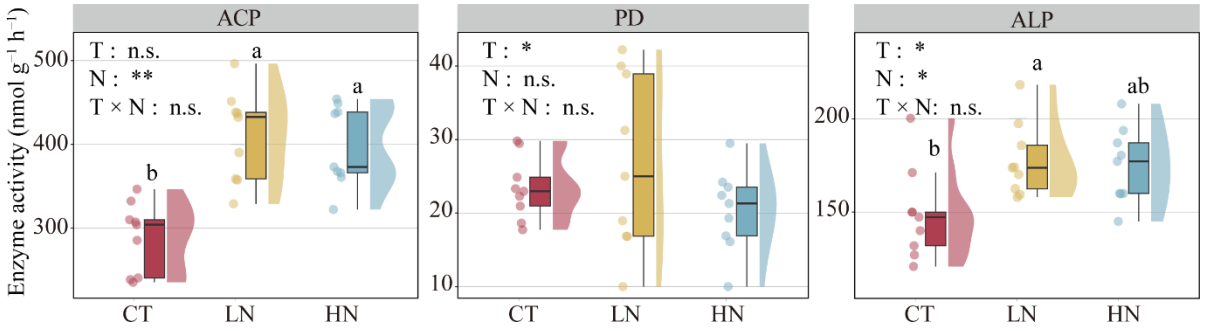
ACP
PD
ALP
Enzyme activity (nmol g⁻¹ h⁻¹)
T : n.s.
N : **
T × N : n.s.
T : *
N : n.s.
T × N : n.s.
T : *
N : *
T × N: n.s.
a
a
b
a
ab
b
CT
LN
HN

837 **Fig. 2**

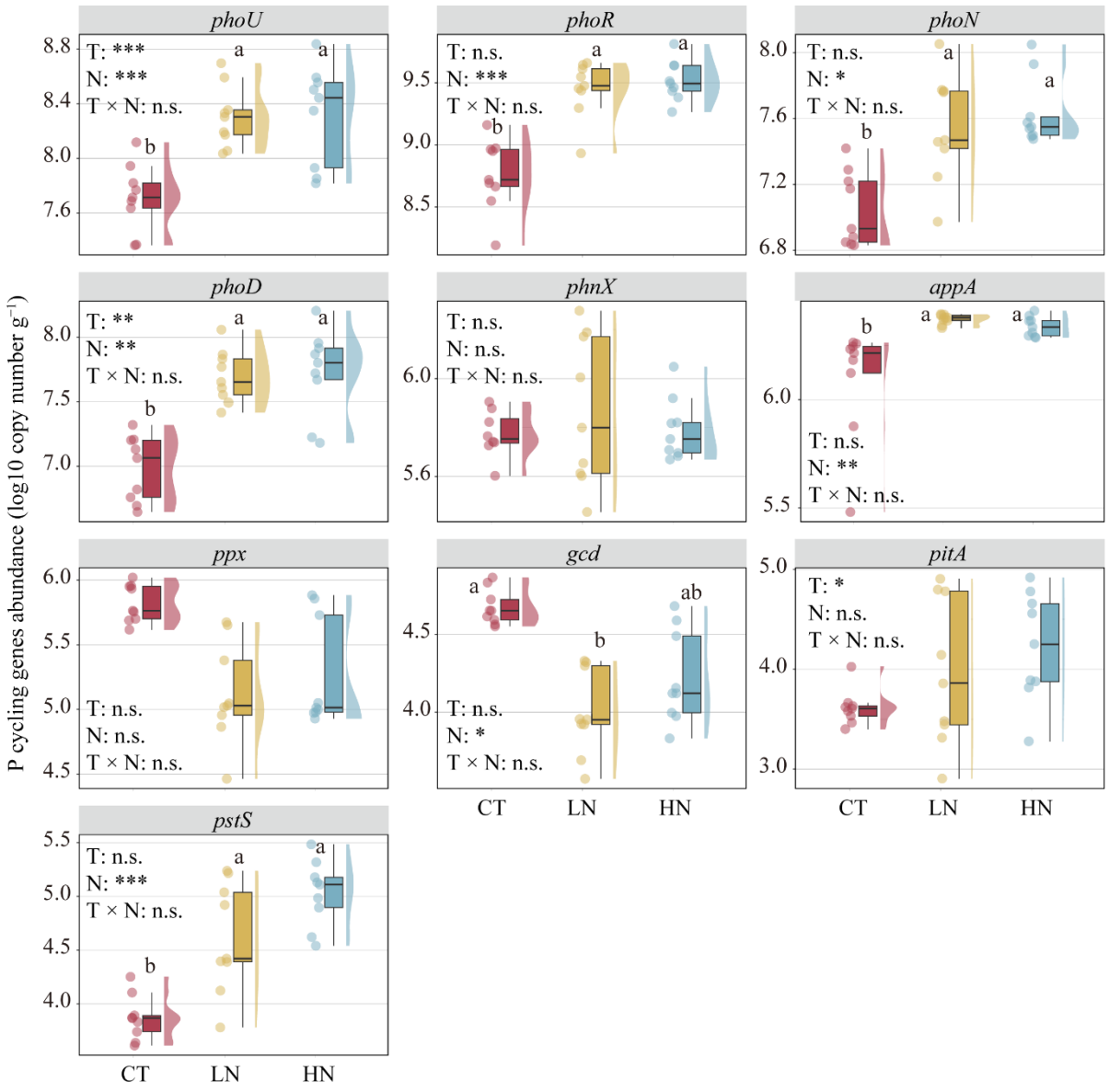
phoU
T: ***
N: ***
T × N: n.s.
phoR
T: n.s.
N: ***
T × N: n.s.
phoN
T: n.s.
N: *
T × N: n.s.
phoD
T: **
N: **
T × N: n.s.
phnX
T: n.s.
N: n.s.
T × N: n.s.
appA
T: n.s.
N: **
T × N: n.s.
ppx
T: n.s.
N: n.s.
T × N: n.s.
gcd
T: n.s.
N: *
T × N: n.s.
pitA
T: *
N: n.s.
T × N: n.s.
pstS
T: n.s.
N: ***
T × N: n.s.
P cycling genes abundance (log10 copy number g⁻¹)
CT
LN
HN

**Fig. 3**

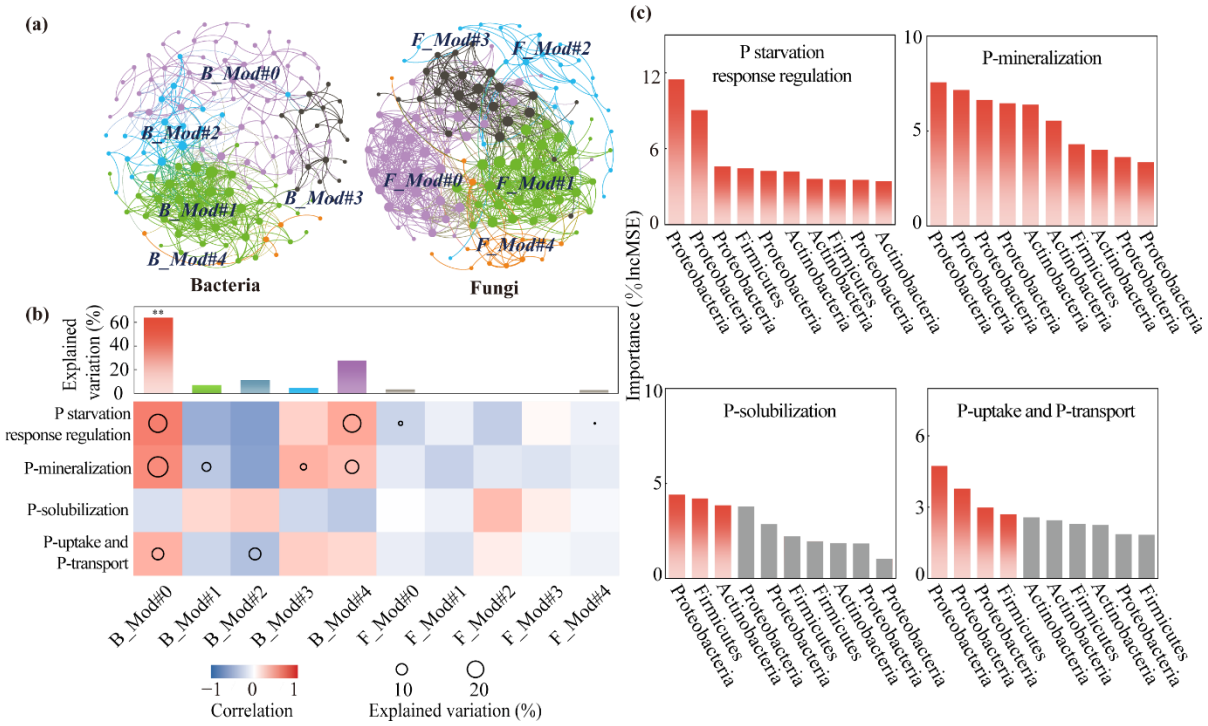
(a)
B_Mod#0
B_Mod#2
B_Mod#1
B_Mod#3
B_Mod#4
Bacteria
F_Mod#3
F_Mod#2
F_Mod#0
F_Mod#1
F_Mod#4
Fungi
(b)
Explained variation (%)
60
40
20
0
**
P starvation response regulation
P-mineralization
P-solubilization
P-uptake and P-transport
B_Mod#0
B_Mod#1
B_Mod#2
B_Mod#3
B_Mod#4
F_Mod#0
F_Mod#1
F_Mod#2
F_Mod#3
F_Mod#4
−1 0 1
Correlation
10
20
Explained variation (%)
(c)
Importance (%IncMSE)
P starvation response regulation
P-mineralization
P-solubilization
P-uptake and P-transport
Proteobacteria
Firmicutes
Actinobacteria

841

842 **Fig. 4**

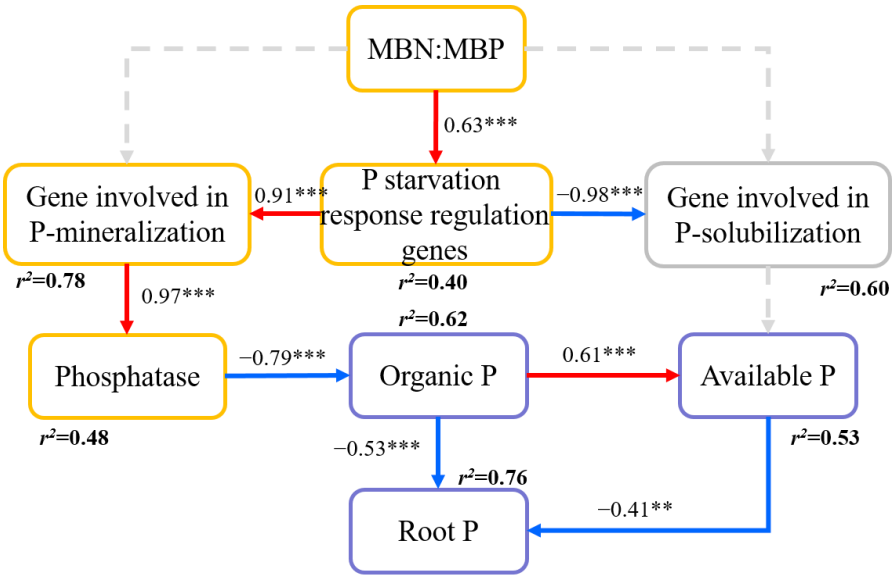


GFI = 1.000, $p$ = 0.591, RMSEA = 0.061, SRMR < 0.001

**Fig. 5**

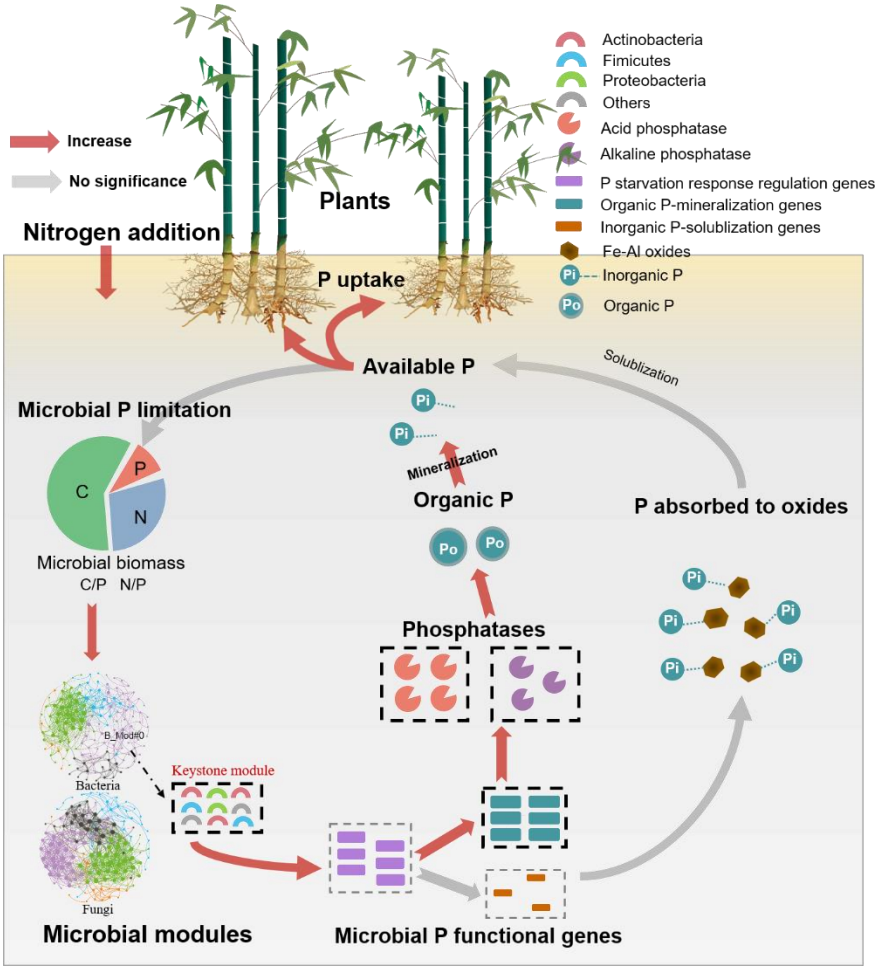
Increase
No significance
Nitrogen addition
Plants
P uptake
Available P
Microbial P limitation
C
P
N
Microbial biomass
C/P N/P
Mineralization
Organic P
Solublization
P absorbed to oxides
Phosphatases
Keystone module
Bacteria
Fungi
Microbial modules
Microbial P functional genes
Actinobacteria
Fimicutes
Proteobacteria
Others
Acid phosphatase
Alkaline phosphatase
P starvation response regulation genes
Organic P-mineralization genes
Inorganic P-solublization genes
Fe-Al oxides
Inorganic P
Organic P

845

846 **Fig. 6**

847 **Table 1.** Variations in microbial biomass and its stoichiometry with N addition.

| Year | Treatment | MBC (mg kg$^{-1}$) | MBN (mg kg$^{-1}$) | MBP (mg kg$^{-1}$) | MBC:MBN | MBC:MBP | MBN:MBP |
|---|---|---|---|---|---|---|---|
| 3rd-year | CT | 780 (156) | 96 (7.8) | 43 (6.5) a | 8.2 (1.5) | 18.5 (3.7) a | 2.3 (0.2) a |
| | LN | 1078 (283) | 79 (8.2) | 45 (8.5) a | 14.1 (4.2) | 25.5 (7.3) a | 1.8 (0.2) a |
| | HN | 1509 (54) | 114 (16.7) | 47 (3.6) a | 13.1 (1.8) | 32.5 (1.5) a | 2.4 (0.2) a |
| 4th-year | CT | 1119 (205) | 104 (9.8) | 69 (4.9)a | 10.5 (0.7) | 16.2 (3.0) b | 1.5 (0.1) b |
| | LN | 966 (128) | 91 (5.8) | 41 (4.1)b | 10.8 (1.1) | 24.6 (5.1) ab | 2.2 (0.2) ab |
| | HN | 1161 (183) | 106 (10.9) | 38 (4.5)b | 11.3 (1.2) | 30.5 (4.4) a | 2.8 (0.2) a |
| 5th-year | CT | 1255(128) | 139 (2.5) | 50 (3.3) a | 8.9 (0.4) | 24.8 (1.3)b | 2.8 (0.1) c |
| | LN | 1140 (147) | 124 (21.3) | 35 (2.1) b | 10.0 (2.5) | 32.6 (4.4)ab | 4.2 (0.3) b |
| | HN | 1277 (74) | 116 (16.2) | 31 (3.6) b | 11.6 (1.4) | 42.1 (5.3)a | 3.7 (0.4) a |
| Repeated measures ANOVA | T | n.s. | * | n.s. | n.s. | * | *** |
| | N | n.s. | n.s. | ** | n.s. | *** | ** |
| | T×N | n.s. | n.s. | * | n.s. | n.s. | ** |

848 *Note:* All values are means ± SE ($n$ = 3). MBC, microbial biomass C; MBN, microbial biomass
849 N; MBP, microbial biomass P; CT, control; LN, low N addition; HN, high N addition. T, time
850 effect; N, N addition effect; T × N, interactive effect of time and N addition. Asterisks (*)
851 indicate a significant difference (* $P$ < 0.05, ** $P$ < 0.01, and *** $P$ < 0.001). n.s., no
852 significance ($P$ > 0.05). When only main effect of N addition or its interactive effect with time
853 was significant at $p$ < 0.05, Duncan's test was used to evaluate the significant differences
854 (indicated by different lowercase letters) among N addition treatments in the same year.

**Highlights**

- N addition reduced soil P availability and intensified microbial P limitation
- N addition activated microbial P starvation response and enhanced expression of P mineralization genes
- B_Mod#0 acts as a keystone phylotype in enhancing functional potential for organic P mineralization
- Organic P mineralization is more important than inorganic P desorption for microbial amelioration of P limitation.

## Declaration of Competing Interest

The authors declare that they have no known competing financial interests or personal relationships that could have appeared to influence the work reported in this paper.